AGU PUBLICATIONS

JGR

Journal of Geophysical Research: Space Physics

RESEARCH ARTICLE
10.1002/2014JA020554

Special Section:
Origins and Properties of Kappa Distributions

Electromagnetic fluctuations of the whistler-cyclotron and firehose instabilities in a Maxwellian and Tsallis-kappa-like plasma

Adolfo F. Viñas[1], Pablo S. Moya[1,2,3], Roberto E. Navarro[3,4], J. Alejandro Valdivia[3], Jaime A. Araneda[4], and Víctor Muñoz[3]

[1]Geospace Physics Laboratory, NASA Goddard Space Flight Center, Greenbelt, Maryland, USA, [2]Department of Physics, Catholic University of America, Washington, District of Columbia, USA, [3]Departamento de Física, Facultad de Ciencias, Universidad de Chile, Santiago, Chile, [4]Departamento de Física, Facultad de Ciencias Físicas y Matemáticas, Universidad de Concepción, Concepción, Chile

Key Points:
- Whistler and firehose fluctuations for thermal and nonthermal distributions
- Results show an increase in the fluctuations level for nonthermal distributions
- Results provide a diagnostic signature of the velocity distribution function

Correspondence to:
A. F. Viñas,
adolfo.vinas@nasa.gov

Citation:
Viñas, A. F., P. S. Moya, R. E. Navarro, J. A. Valdivia, J. A. Araneda, and V. Muñoz (2015), Electromagnetic fluctuations of the whistler-cyclotron and firehose instabilities in a Maxwellian and Tsallis-kappa-like plasma, *J. Geophys. Res. Space Physics*, *120*, 3307–3317, doi:10.1002/2014JA020554.

Received 28 AUG 2014
Accepted 23 MAR 2015
Accepted article online 29 MAR 2015
Published online 15 May 2015

Abstract Observed electron velocity distributions in the Earth's magnetosphere and the solar wind exhibit a variety of nonthermal features which deviate from thermal equilibrium, for example, in the form of temperature anisotropies, suprathermal tail extensions, and field-aligned beams. The state close to thermal equilibrium and its departure from it provides a source for spontaneous emissions of electromagnetic fluctuations, such as the whistler. Here we present a comparative analysis of the electron whistler-cyclotron and firehose fluctuations based upon anisotropic plasma modeled with Maxwellian and Tsallis-kappa-like particle distributions, to explain the correspondence relationship of the magnetic fluctuations as a function of the electron temperature and thermal anisotropy in the solar wind and magnetosphere plasmas. The analysis presented here considers correlation theory of the fluctuation-dissipation theorem and the dispersion relation of transverse fluctuations, with wave vectors parallel to the uniform background magnetic field, in a finite temperature anisotropic thermal bi-Maxwellian and nonthermal Tsallis-kappa-like magnetized electron-proton plasma. Dispersion analysis and stability thresholds are derived for these thermal and nonthermal distributions using plasma and field parameters relevant to the solar wind and magnetosphere environments. Our results indicate that there is an enhancement of the fluctuations level in the case of nonthermal distributions due to the effective higher temperature and the excess of suprathermal particles. These results suggest that a comparison of the electromagnetic fluctuations due to thermal and nonthermal distributions provides a diagnostic signature by which inferences about the nature of the particle velocity distribution function can be ascertained without in situ particle measurements.

1. Introduction

Nonthermal particle velocity distributions that often appear as suprathermal tail extension which decreases as a power law of the velocity are ubiquitous in space plasmas, and they are specially inherent to the solar wind and magnetospheric electron distributions [*Olbert*, 1968; *Vasyliunas*, 1968; *Montgomery*, 1968; *Feldman et al.*, 1975; *Pilipp et al.*, 1987; *Maksimovic et al.*, 1997; *Nieves-Chinchilla and Viñas*, 2008; *Zouganelis*, 2008]. These distributions are remarkably modeled by the well-known Tsallis-kappa-like distribution as a fitting function. It has been suggested that such class of velocity distribution are the resultant of a more general-universal mechanism that generates these stable distributions which exists on many complex-systems such as astrophysical, quantum, biological, economic, and for certainty in space plasma systems [*Tsallis*, 1988; *Gell-Mann and Tsallis*, 2004; *Tsallis and Brigatti*, 2004]. These distributions play an important role in the description of particle acceleration, in defining the thermodynamic or kinetic temperature and in the wave-particle interactions of any plasma system. Among the many fundamental challenging problems of laboratory and astrophysical plasmas, two of the most important are the understanding of the relaxation of collisionless plasmas with nearly isotropic nonthermal velocity distribution functions and the resultant state of nearly equipartition energy density with electromagnetic plasma turbulence. Regardless of the absence of free energy for plasma instabilities, a thermal and nonthermal plasma sustains a small but detectable spontaneous fluctuation level of absorption and emission which arises from the discreteness of the plasma particles, e.g., from the charge and current fluctuations in the plasma. The response of a nonthermal plasma, due to these spontaneous emissions,

is intimately associated to the electric and magnetic field fluctuations which can be described by the well-known fluctuation-dissipation theorem (FDT). Spectral properties of the scattered fluctuating emission provide substantial information about the state of a plasma, and in fact it is one of the most efficient methods of plasma diagnostics used in laboratory fusion research devices and in space plasma measurement [see, e.g., *Meyer-Vernet et al.*, 1986; *Lund et al.*, 1994; *Issautier et al.*, 2001; *Moncuquet et al.*, 2005; *Chapman and Gericke*, 2011; *Meyer-Vernet et al.*, 2013].

Recent analysis of solar wind proton temperature anisotropies observed by the two Faraday Cup instruments of the Solar Wind Experiment (SWE) on the Wind satellite [*Kasper et al.*, 2002] has shown direct correspondence to the measured magnetic fluctuation wave power obtained by the Magnetic Field Investigation [*Bale et al.*, 2009]. Using various years of data, they demonstrated that the observed limit of the proton temperature anisotropy for $T_{\perp p}/T_{\parallel p} < 1$ and $T_{\perp p}/T_{\parallel p} > 1$ is in agreement with the constraints predicted by theory and simulations, as imposed by the firehose and the Alfvén proton-cyclotron instabilities, respectively. Although their results show a clear correspondence between the temperature anisotropies and the magnetic fluctuation near the instability thresholds, their analysis does not provide a complete physical explanation for the magnetic fluctuations within the instability threshold regions. Such explanation, proposed in *Araneda et al.* [2012], *Viñas et al.* [2014], and *Navarro et al.* [2014], can be obtained by a study of the relaxation of thermal and nonthermal plasmas by means of the FDT that describes the state of the system by the linear response of the plasma media to the perturbations from its equilibrium state [e.g., *Callen and Welton*, 1951; *Ichimaru*, 1962; *Sitenko*, 1967]. Despite the fact that we just have a few similar observations for electron temperature anisotropy and magnetic fluctuations [*Stverak et al.*, 2008] as those made by *Bale et al.* [2009] and *Kasper et al.* [2002], we make the conjecture by analogy that similar results should be obtained for the electron physics and the high-frequency magnetic whistler-cyclotron fluctuations. Moreover, the temperature anisotropy analysis described in these works is not only limited to low-frequency ion-driven electromagnetic fluctuations, but it is also applicable to high-frequency electromagnetic waves such as whistler-cyclotron and firehose waves where the plasma is dominated by the electron physics and where the electrons are well represented by nonthermal Tsallis-kappa-like distributions as in the solar wind. These nonthermal Tsallis-kappa-like distributions have been observed more naturally on the solar wind [see *Feldman et al.*, 1975; *Pilipp et al.*, 1987; *Maksimovic et al.*, 1997; *Nieves-Chinchilla and Viñas*, 2008] and magnetospheric electrons [see *Olbert*, 1968; *Vasyliunas*, 1968; *Montgomery*, 1968; *Christon et al.*, 1989] than the protons.

Recently, *Araneda et al.* [2012] and *Viñas et al.* [2014] studied magnetic fluctuations associated with Alfvén and whistler waves, respectively, in isotropic Maxwellian thermal plasmas and showed that heavily damped modes of the dispersion relation constrain the structure of the fluctuation spectra, showing that they play an important role in the emission and absorption of plasma fluctuations, as well as in the emergence of collective modes (plasma waves). However, *Viñas et al.* [2014] results extended the study to Tsallis-kappa-like distributions and showed that the spectral distribution of the fluctuations is not constrained by the heavily damped higher-order modes, suggesting that such signature can be used as a diagnostic to identify from wave properties the nature of the plasma distribution function. *Viñas et al.* [2014] further showed that the zone where the whistler-cyclotron normal modes merge the electromagnetic fluctuations shifts to longer wavelengths as the $\beta_{\parallel}$ increases [see also *Araneda et al.*, 2012]. This merging zone has been interpreted as the beginning of the region where the whistler-cyclotron waves lose their identity and become heavily damped while merging with the fluctuations. *Navarro et al.* [2014] extended some of these ideas to anisotropic but stable bi-Maxwellians, showing that these fluctuations are in qualitative agreement and may explain solar wind observations. Analogously, *Schlickeiser and Yoon* [2012] derived general expressions for the electromagnetic fluctuation spectra in unmagnetized relativistic and nonrelativistic plasmas; however, their study is restricted mainly to the description of aperiodic (purely growing/damped) modes generated by a variety of distribution functions [*Lazar et al.*, 2012; *Schlickeiser and Yoon*, 2012; *Felten et al.*, 2013; *Felten and Schlickeiser*, 2013a, 2013b].

In this paper, we use *Sitenko* [1967] fluctuation theory and use the formalism described by *Schlickeiser and Yoon* [2012] for unmagnetized plasmas, and *Navarro et al.* [2014] and *Navarro et al.* [2015] for magnetized plasmas composed of protons and electrons emphasizing the high-frequency parallel-propagating electron-driven whistler-cyclotron and firehose fluctuations for arbitrary bi-Maxwellian and thermally anisotropic Tsallis-kappa-like distribution functions to explain the correspondence of the temperature anisotropy and threshold of magnetic fluctuations in the solar wind and magnetosphere. We then compare our results to those considered by *Navarro et al.* [2014] for low-frequency Alfvén cyclotron waves and *Viñas*

et al. [2014] for high-frequency whistler waves, respectively, when the spectral κ index tends to infinity and the system becomes isotropic (i.e., Maxwellian).

2. Theory of Electromagnetic Fluctuations in Plasmas

It is well known that any physical quantity that characterizes a macroscopic system which is near equilibrium experiences deviations from its average value. These deviations from the average values are called fluctuations of the physical quantity, and they are determined by the thermodynamical or kinetic temperatures and other macroscopic properties of the system. To describe these fluctuations we introduce correlation functions defined as the averaged values of products of fluctuations of a single or several quantities at different points in space and time. These averaged values are taken over the statistical ensemble that characterizes the state of the system. For the purpose of this work we consider that the electromagnetic fluctuations are the quantities characterizing our system.

In considering the fluctuation-dissipation theorem (FDT) and the Tsallis-kappa-like velocity distribution we must point out a basic caveat in the analysis. Our magnetic fluctuation calculations with the FDT theory follows the standard Hamiltonian approach used by *Ichimaru* [1962], *Sitenko* [1967], and more recently by *Navarro et al.* [2014], in which the linear response of the ensemble average of the electromagnetic fluctuations is connected to the plasma response function via the dielectric response of the plasma medium. This approach does not require invoking any entropy principle of classical thermodynamics. In this framework, which follows the traditional method of plasma physics, the dielectric response of the plasma is determined directly from the linearized Vlasov-Maxwell systems of equations, which are, in general, represented in terms of unspecified arbitrary and nearly equilibrium velocity distributions representing the "average" ensemble particle distribution. Generally, these distributions have been assumed to be bi-Maxwellian or a superposition of bi-Maxwellian distributions. In our calculations we have preassumed that the dielectric response is derived in terms of an arbitrary unspecified nearly equilibrium distribution and the systems of interest are the solar wind-magnetosphere. These systems comprised a plasma, where long-range (long-time memory and long correlations) interaction prevails, we can otherwise assume a Tsallis-kappa-like particle distribution in its equilibrium. Moreover, both the fluctuation-dissipation theorem studied in this paper and the Tsallis-kappa-like distribution approaches the standard FDT theory [e.g., *Ichimaru*, 1962; *Sitenko*, 1967] and the Maxwellian distribution in the limit as kappa approaches infinity, respectively. However, it is important to emphasize that this is an ansatz since the Tsallis-kappa-like distribution has been posed in a different formalism of the fluctuation dissipation theorem for nonextensive statistical mechanics proposed by *Chame and de Mello* [1994] and also *Rajagopal* [1996].

In this section we estimate the magnetic fluctuations power spectrum when the plasma is represented by a bi-Maxwellian thermal distribution and later for the more general case of a nonthermal distribution modeled by a Tsallis-kappa-like distribution function. We use the statistical ensemble average of the magnetic field fluctuations through their deviations from the mean values to describe the state of the plasma by the dielectric response of the system. Since the mean value of the fluctuations is equal to zero by definition and the plasma medium is spatially homogeneous, therefore, only nearly stationary states of the system are involved in the correlation. Thus, the quadratic correlation (i.e., nonlinear second-order correlators) function depends only on the relative distance and on the absolute value of the time segment between the points at which the fluctuations are examined. These correlations are ensemble average products of fluctuations that are further described at particular wavelengths and frequencies in the ω-$\mathbf{k}$ Fourier domain. Following standard second-order correlation procedure, the classical spectral power distribution of electric field fluctuations per species s in a magnetized nonisothermal and homogeneous anisotropic plasma can be generally expressed [see *Sitenko*, 1967] in terms of the fluctuation-dissipation theorem:

$$\left\langle \delta E_i \delta E_j^* \right\rangle^{(s)}_{(\omega,\vec{k})} = 4\pi i \frac{k_B T_{\perp s}}{\omega} \Lambda^{-1}_{(0)} \left(\Lambda^{-1}_{jm} \chi^{(s)}_{mi} - \chi^{(s)*}_{im} \Lambda^{-1*}_{mj} \right), \tag{1}$$

where ω is the frequency of the fluctuations, Λ^{-1}_{ij} are the components of the inverse of the dispersion tensor, $\Lambda^{-1}_{(0)}$ is a diagonal inverse dispersion tensor of free space (vacuum), $\chi^{(s)}$ is the electromagnetic susceptibility tensor per species s, $T_{\perp s}$ is the species perpendicular temperature and k_B is the Boltzmann constant. The bracket $\langle \cdots \rangle$ represents the statistical space-time ensemble average for each frequency and wave vector [see also *Navarro et al.*, 2015].

For an anisotropic nonisothermal plasma and in the limit of parallel propagation we can express the trace of this equation in terms of the transverse magnetic fluctuations as follows:

$$\left\langle |\delta B_\perp|^2 \right\rangle_{(\omega,k_\parallel)} = \left\langle \delta B_\perp \cdot \delta B_\perp^* \right\rangle_{(\omega,k_\parallel)} = \frac{8\pi}{\omega} \mathrm{Tr} \left\{ \Lambda_{(0)}^{-1} \ \mathrm{Im} \left[\sum_s \left(\mathrm{T}_{\perp(s)} \chi_\perp^{(s)} \right) \Lambda_\perp^{-1*} \right] \right\} \tag{2}$$

using the Maxwell-Faraday equation, since for parallel propagation $\left\langle |\delta B_\parallel|^2 \right\rangle = 0$, and summing over all plasma species. Here Λ_{mj}^{-1*} is understood to be given by the conjugate inverse parallel dispersion tensor defined below (see equation (4)) which can be expressed as the ratio of its cofactor matrix divided by its determinant, e.g., $\Lambda_{mj}^{-1} = \mathrm{CoFac}\left(\Lambda_{mj}\right)/|\Lambda|$.

Rewriting this final equation in dimensionless units results in the following:

$$\left\langle |\delta \bar{B}_\perp|^2 \right\rangle_{(\omega,k_\parallel)} = \frac{\eta^2}{(1-\eta^2)} \frac{|\Omega_e|}{\omega} \mathrm{Tr} \left\{ \mathrm{Im} \left[\sum_s \left(\Gamma_s \bar{\beta}_{\parallel s} \chi_\perp^{(s)} \right) \Lambda_\perp^{-1} \right] \right\}, \tag{3}$$

where $\eta = ck_\parallel/\omega$ is the index of refraction, $\Gamma_s = T_{\perp s}/T_{\parallel s}$ is the temperature anisotropy for each species, and $\bar{\beta}_{\parallel s} = 8\pi n_0 k_B T_{\parallel s}/B_0^2$ is a plasma beta based on the total density n_0, representing only the species temperature.

The linearized dispersion tensor $\Lambda_{ij}(\omega, \mathbf{k})$ is obtained from the Fourier-Laplace transformed Vlasov-Maxwell equations which yields

$$\mathbf{\Lambda}(\omega, \mathbf{k}) = \Lambda_{(0)} + \boldsymbol{\varepsilon}(\mathbf{k}, \omega), \tag{4}$$

where we have defined the free space dispersion tensor $\Lambda_{(0)}$ as follows:

$$\Lambda_{(0)} = \mathbf{I} - \eta^2 \left(\mathbf{I} - \frac{\mathbf{kk}}{k^2} \right). \tag{5}$$

The electromagnetic response of the plasma medium is completely described in terms of the plasma dielectric permittivity tensor

$$\boldsymbol{\varepsilon}(\mathbf{k}, \omega) = \sum_s \chi^{(s)}, \tag{6}$$

which depends on the susceptibilities $\chi_{ij}^{(s)}$ of the various species, the complex frequency ω, and the wave vector $\mathbf{k}$. The dispersion relation that determines the frequencies $\omega = \omega(\mathbf{k})$, of the normal modes, is given from the condition that $\det(\Lambda) = 0$ (for details, see *Viñas et al.*, 2014 [2014]). For propagation parallel to $\mathbf{B}_0$, and for a plasma composed of parallel drifting electrons and protons that obey the bi-Maxwellian particle velocity distribution function given by:

$$F_s\left(v_\parallel, v_\perp\right) = \frac{1}{\pi^{3/2}\alpha_{\parallel s}\alpha_{\perp s}^2} \exp\left[-\frac{\left(v_\parallel - U_{\parallel s}\right)^2}{\alpha_{\parallel s}^2} - \frac{v_\perp^2}{\alpha_{\perp s}^2} \right], \tag{7}$$

the dielectric permittivity tensor in nondiagonal form becomes

$$\begin{aligned}
\varepsilon_{11}(\omega, k_\parallel) &= \frac{1}{2} \sum_s \frac{\omega_{\mathrm{ps}}^2}{\omega^2} \left[2\left(\Gamma_s - 1\right) - \Gamma_s \left(\bar{\xi}_s^- Z(\xi_s^-) + \bar{\xi}_s^+ Z(\xi_s^+) \right) \right], \\
\varepsilon_{12}(\omega, k_\parallel) &= \frac{i}{2} \sum_s \frac{\omega_{\mathrm{ps}}^2}{\omega^2} \left[\Gamma_s \left(\bar{\xi}_s^- Z(\xi_s^-) - \bar{\xi}_s^+ Z(\xi_s^+) \right) \right], \\
\varepsilon_{33}(\omega, k_\parallel) &= -2 \sum_s \frac{\omega_{\mathrm{ps}}^2}{k_\parallel^2 \alpha_{\parallel s}^2} \left[1 + \xi_s Z\left(\xi_s\right) \right],
\end{aligned} \tag{8}$$

and

$$\varepsilon_{13} = \varepsilon_{23} = \varepsilon_{31} = \varepsilon_{32} = 0 \text{ and }, \varepsilon = \varepsilon_{11} \text{ and } \varepsilon_{21} = -\varepsilon_{12}, \tag{9}$$

where we have defined; given by

$$\xi_s = \frac{(\omega - k_\parallel U_{\parallel s})}{k_\parallel \alpha_{\parallel s}}, \ \xi_s^\pm = \xi_s \mp \frac{\Omega_s}{k_\parallel \alpha_{\parallel s}}, \ \bar{\xi}_s^\pm = \xi_s \mp \frac{\Omega_s \left(1 - \Gamma_s^{-1}\right)}{k_\parallel \alpha_{\parallel s}}. \tag{10}$$

In equation (8), $\omega_{ps}^2 = 4\pi n_s q_s^2/m_s$ is the squared plasma frequency; $\Omega_s = q_s B_0/(m_s c)$ is the cyclotron frequency, with n_s, q_s, and m_s the density, charge, and mass of the species s, respectively; and c is the speed of light. The parameters $\alpha_{\|s} = \sqrt{2\kappa_B T_{\|s}/m_s}$ and $\alpha_{\perp s} = \sqrt{2\kappa_B T_{\perp s}/m_s}$ are the parallel and perpendicular thermal velocities, respectively. $Z(\xi)$ is the traditional Fried-Conte plasma dispersion function [*Fried and Conte*, 1961]. The generalized expression for the magnetic fluctuations in equation (2) reduces to that of *Sitenko* [1967] in the isothermal and isotropic limit.

Analogously, a plasma composed of parallel drifting electrons and protons that obey the thermally anisotropic Tsallis-kappa-like particle velocity distribution function [*Tsallis*, 1988; *Tsallis and Brigatti*, 2004; *Tsallis*, 2009] is given by:

$$F_{s\kappa}\left(v_{\|}, v_{\perp}\right) = A_{s\kappa}\left[1 + \frac{1}{\kappa}\left(\frac{\left(v_{\|} - U_{\|s}\right)^2}{\alpha_{\|s}^2} + \frac{v_{\perp}^2}{\alpha_{\perp s}^2}\right)\right]^{-(\kappa+1)},$$
$$A_{s\kappa} = \frac{1}{\pi^{3/2}\alpha_{\|s}\alpha_{\perp s}^2}\frac{\Gamma(\kappa+1)}{\kappa^{3/2}\Gamma(\kappa-1/2)}. \tag{11}$$

Here the parameter κ represents the degree of nonthermal effects. When κ is positive and small, the velocity distribution in equation (11) represents an effectively hotter distribution than a bi-Maxwellian in the form of a suprathermal extension that decreases as a power law, whereas for κ large and approaching infinity, the effective temperature reduces to that of a bi-Maxwellian distribution. This effective temperature T_κ of a Tsallis-kappa-like distribution can be defined in terms of the Maxwellian temperature T by obtaining the second moment of the distribution function equation (11) to yield

$$T_\kappa = \frac{\kappa}{\kappa - 3/2}T, \tag{12}$$

which is a well-defined larger effective temperature for all $\kappa > 3/2$.

Substituting equation (11) into equations (4)–(6), we can write the perpendicular dispersion tensor as follows:

$$\varepsilon_{11}(\omega, k_{\|}) = \frac{1}{2}\sum_s \frac{\omega_{ps}^2}{\omega^2}\left[2\left(\Gamma_s - 1\right) - \Gamma_s\left(\bar{\xi}_s^- Z_\kappa(\xi_s^-) + \bar{\xi}_s^+ Z_\kappa(\xi_s^+)\right)\right],$$
$$\varepsilon_{12}(\omega, k_{\|}) = \frac{i}{2}\sum_s \frac{\omega_{ps}^2}{\omega^2}\left[\Gamma_s\left(\bar{\xi}_s^- Z_\kappa(\xi_s^-) - \bar{\xi}_s^+ Z_\kappa(\xi_s^+)\right)\right], \tag{13}$$
$$\varepsilon_{33}(\omega, k_{\|}) = -\frac{2\kappa - 1}{\kappa}\sum_s \frac{\omega_{ps}^2}{k_{\|}^2\alpha_{\|s}^2}\left[1 + \xi_s^\kappa Z_{\kappa+1}\left(\xi_s^\kappa\right)\right],$$

where the arguments ξ_s and $\xi_s^\pm$ have been defined in equation (10),

$$\xi_s^\kappa = \sqrt{\frac{\kappa+1}{\kappa}}\left[\frac{(\omega - k_{\|}U_{\|})}{k_{\|}\alpha_{\|s}}\right], \tag{14}$$

and the modified kappa dispersion function is given by

$$Z_\kappa(\xi) = \frac{\Gamma(\kappa)}{\pi^{1/2}\kappa^{1/2}\Gamma(\kappa - 1/2)}\int_{-\infty}^{+\infty}\frac{dt}{(t-\xi)}\left[1 + \frac{t^2}{\kappa}\right]^{-\kappa}, \quad \mathrm{Im}(\xi) > 0. \tag{15}$$

For $\kappa > 1/2$, the function $Z_\kappa(\xi)$ can be written in terms of the Gauss hypergeometric function ${}_2F_1$:

$$Z_\kappa(\xi) = i\frac{\kappa - 1/2}{\kappa^{3/2}}\,{}_2F_1\left[1,\ 2\kappa;\ \kappa + 1;\ \frac{1}{2}\left(1 - \frac{\xi}{i\sqrt{\kappa}}\right)\right]. \tag{16}$$

Here $Z_\kappa(\xi)$ is the analogous plasma dispersion function for a kappa-like distribution as defined by *Summers and Thorne* [1991] and *Mace and Sydora* [2010].

The magnetic fluctuations spectrum when the plasma is represented by a Tsallis-kappa-like nonthermal anisotropic distribution is slightly modified compared to equation (3) above for the bi-Maxwellian. In this case

the temperature is expressed in terms of the effective temperature given by equation (12); thus, the resultant magnetic fluctuation spectrum (in dimensionless form) becomes

$$\left\langle |\delta \bar{B}_{\perp}|^2 \right\rangle_{(\omega,k_{\parallel})} = \frac{\eta^2}{(1-\eta^2)} \frac{|\Omega_e|}{\omega} \mathrm{Tr} \left\{ \mathrm{Im} \left[\sum_s \left(\frac{\kappa_s}{\kappa_s - 3/2} \Gamma_s \bar{\beta}_{\parallel s} \chi_{\perp}^{(s)} \right) \Lambda_{\perp}^{-1} \right] \right\}, \tag{17}$$

which clearly implies that the fluctuations will be enhanced by the effective temperature for a Tsallis-kappa-like distributions at a given κ value and fixed plasma conditions.

3. Numerical Results

In this section we present the results of the electromagnetic whistler-cyclotron and firehose fluctuation power calculated from equations (3) and (17) for a bi-Maxwellian and a Tsallis-kappa-like electron-proton plasma distribution functions, respectively. The results consider two typical plasma environment cases: (1) the solar wind region where $\omega_{\mathrm{pe}}/|\Omega_e| \simeq 100$ and (2) the magnetosphere domain where $\omega_{\mathrm{pe}}/|\Omega_e| \simeq 5$. The calculation of the spectral power is carried out by considering a plasma with an isotropic proton distribution represented by a fixed $\bar{\beta}_p = 0.1$. The electron temperature and anisotropy were varied in the range of $0.01 \leq \bar{\beta}_e \leq 10$ and $0.1 \leq \Gamma_e \leq 10$, respectively. The dispersion relation for the electron-proton plasma is then evaluated for these parameters to estimate the right-hand side of equations (3) and (17). Since the calculations of the spectral power are in the Fourier spaces $(k_{\parallel}, \omega)$, we integrated equations (3) and (17) in both frequency and wavelength for the range $-5 \leq k_{\parallel}\lambda_e \leq 5$ and $-5 \leq \omega/|\Omega_e| \leq 5$, respectively, to estimate the total power in configurational space (since they are equivalent by Parseval's theorem) given by the trace of the spectral power spectrum matrix $|\delta \bar{B}_{\perp}|^2 = \sum \left(|\delta B_x|^2 + |\delta B_y|^2 \right)$ in dimensionless units in the following form:

$$W = \int \mathrm{d}\omega \, \mathrm{d}k_{\parallel} \, |\delta \bar{B}_{\perp}|^2. \tag{18}$$

Here $\lambda_e = c/\omega_{\mathrm{pe}}$ is the electron inertial length and we have taken $U_{\parallel s} = 0$ for both species.

Figure 1a shows contour plots of the maximum growth rate of the dominant modes of the system for typical solar wind parameters assuming a bi-Maxwellian electron-proton plasma. Calculations of the dispersion relation show that there are two relevant domains of the thermal anisotropy given by $1 \leq \Gamma_e \leq 10$, where the whistler cyclotron dominates and $0.1 \leq \Gamma_e \leq 1$, where the firehose left-handed waves dominate, for the full range of the electron temperatures $0.01 \leq \bar{\beta}_e \leq 10$ [see, e.g., *Viñas et al.*, 2014]. The results for the right-handed whistler-cyclotron waves show a clear increase of the growth rate as the anisotropy increases from $1 \leq \Gamma_e \leq 10$ and β_e increases. Similarly, the growth rate of the left-handed firehose waves increases as the anisotropy decreases for the range $0.1 \leq \Gamma_e \leq 1$ when β_e increases. Two threshold growth contour levels are indicated by the dashed lines at $\gamma/|\Omega_e| = 10^{-4}$ and $\gamma/|\Omega_e| = 10^{-3}$ for both modes. Growth rates smaller than $\gamma/|\Omega_e| \leq 10^{-4}$ have been set to the black color level to represent linear quasi-stable (near equilibrium) regimes due to the fact that the time scales for the development of the instabilities are much longer compared to correlation times. Figure 1a clearly shows the two instability domains where the whistler-cyclotron and the firehose dominates. The contour plots of Figure 1b illustrate the corresponding results for the total spectral amplitude power (W) of the electromagnetic whistler-cyclotron and firehose fluctuations calculated from equation (18). This figure also shows that the whistler-cyclotron modes have more power than the firehose modes. This is consistent with their corresponding growth rates, since the whistler-cyclotron growth is generally higher than the firehose growth rates. Because the threshold boundary in the maximum growth rate as well as the total spectral power of the whistler-cyclotron and firehose fluctuations in the solar wind case are shifted to higher β_e values and their respective thermal anisotropies are in different regimes we show these contour plots on a linear scale of the temperature $\bar{\beta}_e$ and thermal anisotropy Γ_e. However, for comparison purposes only, we show the same plots in the logarithm scale (see Figure 2). Figure 2 shows identical plots to Figure 1 but in the log scale which emphasizes what we have discussed on Figure 1. The threshold maximum growth contour at $\gamma/|\Omega_e| = 10^{-4}$ is superposed in Figure 1b and in Figure 2b (see dashed black line) and the color contours have been suppressed (set to white color) to illustrate that the spectral power amplitude is the largest above these levels for both whistler-cyclotron and firehose instabilities. Without real observations of the solar wind magnetic fluctuations versus temperature and thermal anisotropy of electrons, it is difficult to test the theoretical dependence of the whistler-cyclotron and firehose instabilities against the thermal electron anisotropies, as *Bale et al.* [2009] and *Kasper et al.* [2002] have done for Alfvén cyclotron and Alfvén firehose waves. Particularly,

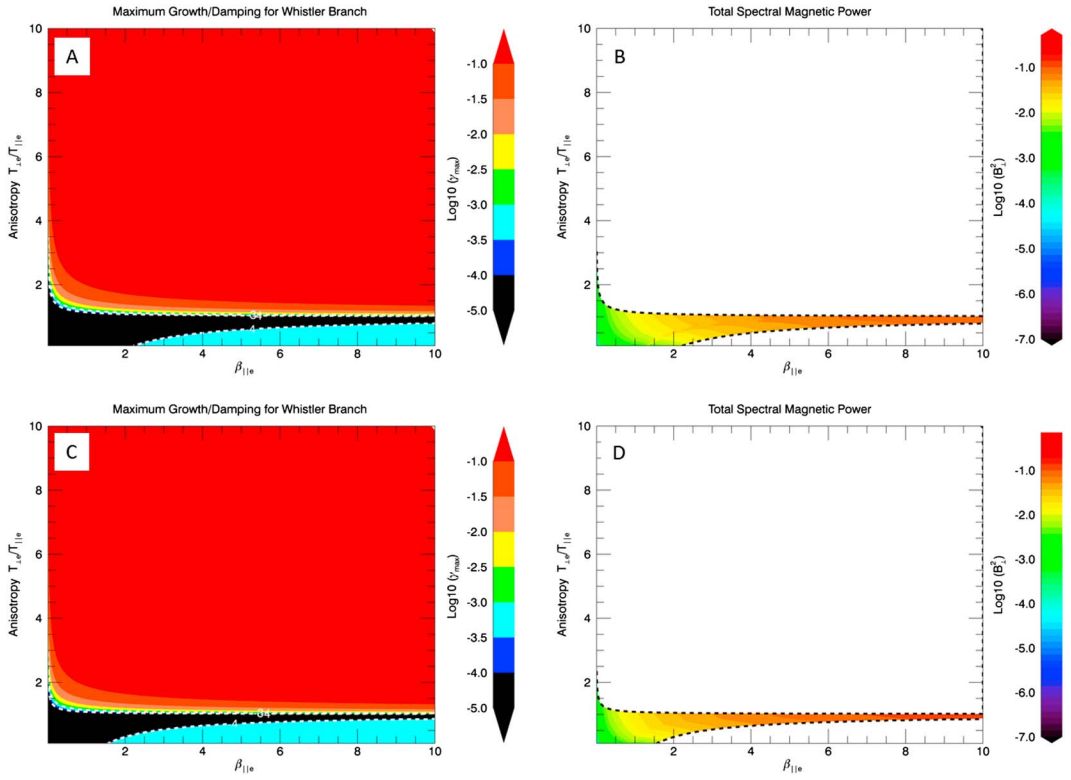

Figure 1. Solar wind maximum growth and total spectral power of magnetic fluctuations for a bi-Maxwellian and anisotropic Tsallis-kappa-like distributions for the case of $\omega_{pe}/|\Omega_e| = 100$ in linear scale. (a) Maximum growth rate and (b) magnetic fluctuation power for a bi-Maxwellian distribution. (c) Maximum growth rate and (d) magnetic fluctuation power for a Tsallis-kappa-like distribution.

if the observations are in the regime below $\gamma/|\Omega_e| \leq 10^{-4}$ corresponding to the lowest power levels of the whistler-cyclotron and firehose waves. *Stverak et al.* [2008] showed some preliminary observations of the electron whistler-cyclotron and firehose instabilities as a function of the temperature and the thermal anisotropies of the electrons (see Figures 5 and 6 of their paper). Their results were based on the separation of the core and halo electron populations resulting from a model-dependent approach analogous to our Maxwellian and Tsallis-kappa-like electron velocity distribution representation of the full distribution. But their results show some ambiguities since they presented their analysis in terms of the occurrence rates rather than the magnetic fluctuations.

In Figures 1c and 1d (as well as in Figures 2c and 2d in logarithmic scale) we show similar results of the growth rates and total spectral amplitude whistler-cyclotron and firehose fluctuations for the case of a Tsallis-kappa-like electron-proton nonthermal plasma in the solar wind with κ values given by $\kappa_e = 5$ for electrons and $\kappa_p = 15$ for protons (i.e., essentially Maxwellian protons). Similar contour plots of the corresponding maximum growth rates and power spectral amplitude of the electromagnetic whistler-cyclotron and firehose fluctuations for the same temperature and anisotropy range of $0.01 \leq \tilde{\beta}_e \leq 10$ and $0.1 \leq \Gamma_e \leq 10$ are presented. Note that the maximum growth threshold contour boundary in Figure 1c (see white dashed line) shifts to smaller values of $\tilde{\beta}_e$ and Γ_e indicating that the Tsallis-kappa-like model is more unstable over a wider dynamic range than the Maxwellian case (see Figure 1a for comparison). Moreover, the spectral power amplitude fluctuations are consistently larger because of the higher effective temperature T_κ (for both parallel and perpendicular) of the plasma and the lack of the higher-order modes bounded structure in the Fourier domain [*Viñas et al.*, 2014]. A comparison between Figures 1d for the Tsallis-kappa-like and Figures 1b for the bi-Maxwellian distributions shows that the enhancement of the suprathermal tails increases the fluctuation levels as shown by the shift in the threshold boundary line in these figures. This again is indicative of the effect of the effective higher temperature of the Tsallis-kappa-like distribution function which increases the fluctuation amplitudes, and therefore, these extended power law distributions have more free energy available.

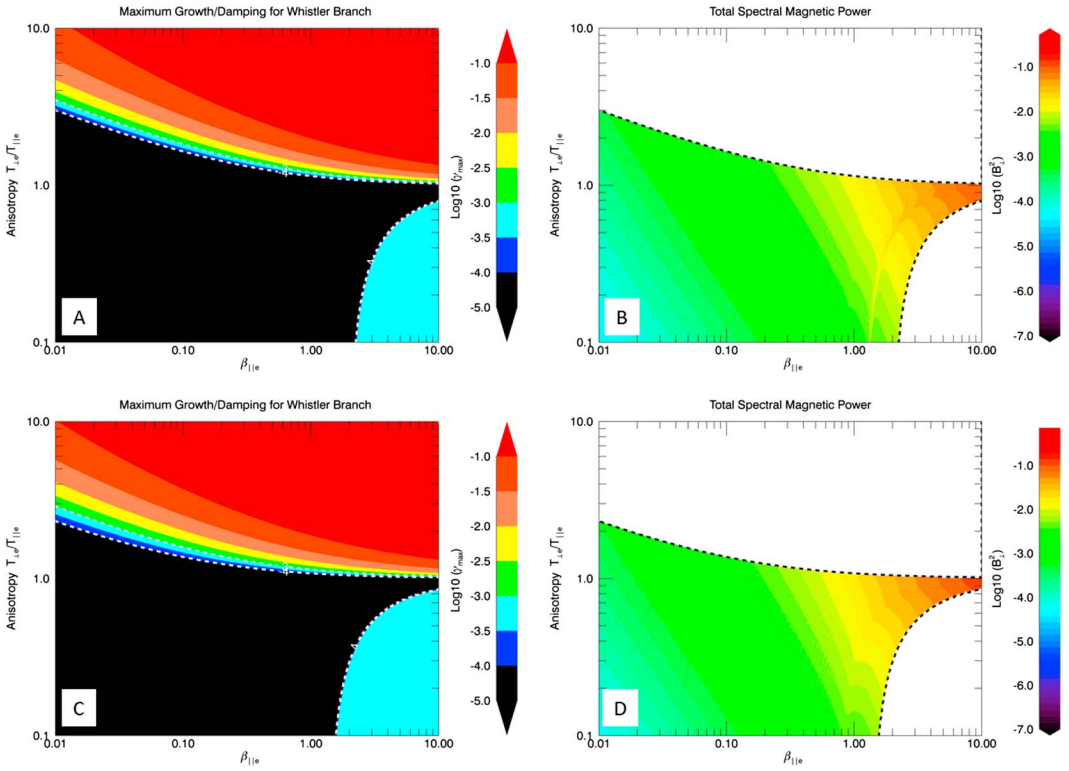

Figure 2. Solar wind maximum growth and total spectral power of magnetic fluctuations for a bi-Maxwellian and anisotropic Tsallis-kappa-like distributions for the case of $\omega_{pe}/|\Omega_e| = 100$ in logarithmic scale. (a) Maximum growth rate and (b) magnetic fluctuation power for a bi-Maxwellian distribution. (c) Maximum growth rate and (d) magnetic fluctuation power for a Tsallis-kappa-like distribution.

Similar results were carried out for the case of typical parameters (i.e., $\omega_{pe}/|\Omega_e| = 5$) in the magnetosphere. In Figure 3a we present contour plots of the maximum growth rate of the dominant modes of the system for typical magnetospheric parameters assuming a bi-Maxwellian electron-proton plasma. The calculations of the dispersion relation reveal again two relevant domains of the thermal anisotropy ($1 \leq \Gamma_e \leq 10$) for the whistler-cyclotron and the firehose left-handed waves ($0.1 \leq \Gamma_e \leq 1$) which are present for the full range of the electron temperatures $0.01 \leq \bar{\beta}_e \leq 10$ [*Viñas et al.*, 2014]. Two threshold growth contour levels are indicated by the dashed lines at $\gamma/|\Omega_e| = 10^{-4}$ and $\gamma/|\Omega_e| = 10^{-3}$ for both the whistler-cyclotron and firehose modes. Growth rates smaller than $\gamma/|\Omega_e| \leq 10^{-4}$ represent stable near-equilibrium regimes. The contour plot of Figure 3b illustrates the corresponding results for the total spectral amplitude power of the electromagnetic whistler-cyclotron and firehose fluctuations. The threshold maximum growth contour at $\gamma/|\Omega_e| = 10^{-4}$ is superposed in Figure 3b (see solid black line) to illustrate that the spectral power amplitude is the largest above this level. Thus, the power spectral amplitudes below $\gamma/|\Omega_e| \leq 10^{-4}$ corresponding to the power level of the electron whistler-cyclotron and firehose fluctuations show a clear correspondence between the temperature anisotropies and the magnetic fluctuation near the instability thresholds boundaries. Figures 3a and 3b for the magnetospheric case clearly show that the whistler-cyclotron instability extends to smaller values of the electron beta, suggesting that it is more susceptible for excitation compared to the solar wind case.

In Figures 3c and 3d we show the results of the growth rates and total spectral power for whistler-cyclotron and firehose fluctuations in the case of a Tsallis-kappa-like electron-proton nonthermal plasma in the magnetosphere with κ values given by $\kappa_e = 5$ and $\kappa_p = 15$. Similar contour plots of the corresponding maximum growth rates and power spectral amplitude of the electromagnetic whistler-cyclotron and firehose fluctuations for the same temperature and anisotropy range of $0.01 \leq \bar{\beta}_e \leq 10$ and $0.1 \leq \Gamma_e \leq 10$ are presented. Note that the spectral power amplitude fluctuations are larger because of the higher effective temperature T_κ of the plasma. A similar comparison between Figure 3b for the bi-Maxwellian and Figure 3d for the Tsallis-kappa-like distributions shows that the enhancement of the suprathermal tails increases the fluctuation levels as shown

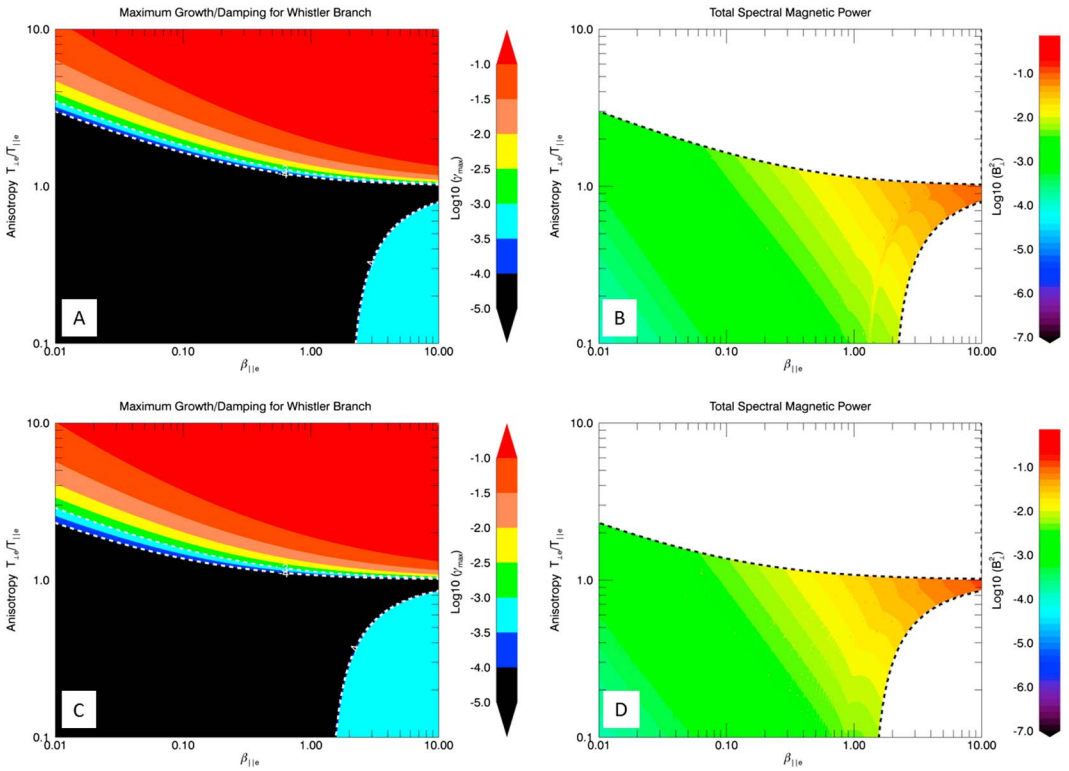

Figure 3. Magnetospheric maximum growth and total spectral power of magnetic fluctuations for a bi-Maxwellian and anisotropic Tsallis-kappa-like distributions for the case of $\omega_{pe}/|\Omega_e| = 5$. (a) Maximum growth rate and (b) magnetic fluctuation power for a bi-Maxwellian distribution. (c) Maximum growth rate and (d) magnetic fluctuation power for a Tsallis-kappa-like distribution.

by the shift in the threshold boundary line in these figures. This again is indicative of the effect of the effective higher temperature due to the extended tails of the Tsallis-kappa-like distribution function.

Similar to the solar wind case, an increase of the growth rate and the magnetic fluctuation wave spectral power of the whistler-cyclotron waves as the anisotropy increases from $1 \leq \Gamma_e \leq 10$ and β_e increases; whereas similar increases occurred for the growth rate of the left-handed firehose waves as the anisotropy decreases for the range $0.1 \leq \Gamma_e \leq 1$ when β_e increases. Analogous to the solar wind case, these increases in the total spectral power and growth rates of the magnetic fluctuations occurred for both the bi-Maxwellian (i.e., equation (3)) and Tsallis-kappa-like (i.e., equation (17)) distributions.

4. Summary and Discussion

We have estimated numerically the total spectral power of the electromagnetic whistler-cyclotron and firehose fluctuations in thermal (bi-Maxwellian) and nonthermal (anisotropic Tsallis-kappa-like) plasmas near quasi-equilibrium as a function of the electron parallel temperature and thermal anisotropy for two typical astrophysical plasma systems such as the solar wind and magnetosphere. Our results indicate that the correspondence between the electron thermal anisotropy and the electromagnetic fluctuations near the instability thresholds of the right-handed whistler-cyclotron and this relationship between the electron temperature, the thermal anisotropy, and the electromagnetic fluctuations near the instability thresholds of the right-handed whistler-cyclotron and left-handed firehose instabilities appear to be well explained by the fluctuation-dissipation theory. The fluctuation-dissipation results shown for the Tsallis-kappa-like velocity distribution seem to be consistent with those for the bi-Maxwellian distribution when κ approaches infinity for both plasma system environments. However, it will be interesting to also use the generalized approach of the FDT theory of nonextensive statistical mechanics of *Chame and de Mello* [1994] to ascertain which framework is more consistent.

The results shown here are expected to provide sufficient motivation for researchers to investigate the thermal relaxation of magnetic fluctuation in the higher-frequency electron whistler-cyclotron and firehose regimes and to present evidence or lack thereof of the correspondence or not of such fluctuations with the electron thermal anisotropy in the solar wind and magnetosphere environments, as it has already been done at the proton scales in *Bale et al.* [2009] and *Navarro et al.* [2014] for solar wind conditions. The only electron observation results currently available are those of *Stverak et al.* [2008] that show similar threshold correspondence boundaries on the number of events versus the temperature and thermal anisotropy of electrons in the solar wind. Unfortunately, such correspondence is at most ambiguous since it was not calculated on the basis of magnetic fluctuations that will render their results more physical than statistical.

Our results further show that the fluctuation spectrum is enhanced in regions where there are suprathermal particles, and the particle velocity distribution is characterized by extended power law tails as those modeled by the Tsallis-kappa-like distribution. The enhancement effect of the spectrum is more pronounced as κ decreases. This result is consistent with the conclusions reached by *Viñas et al.* [2014], where they showed that the electromagnetic fluctuations are not confined by the heavily damped higher-order linear modes in a nonthermal Tsallis-kappa-like plasma. Independent of the value of κ, any instability in the whistler-cyclotron or firehose branch could emerge in these zones if free energy is available [*Viñas et al.*, 2014]. In a thermal Maxwellian plasma these fluctuations usually appear to be constrained within zones bounded by these heavily damped linear modes [*Araneda et al.*, 2012; *Viñas et al.*, 2014]. Thus, this result suggests a diagnostic signature by using remote sensing of the plasma waves fluctuations, which can be used to ascertain the nature of the particle velocity distribution function without in situ particle measurements. This by no means suggests that in situ particle measurements are not required but emphasizes the importance of plasma wave diagnostics and that plasma wave fluctuations observations can provide inferences [e.g., *Viñas et al.*, 2005] about the particle velocity distribution and some of its macroscopic parameters when particle measurements are unavailable.

As shown for the solar wind protons, we expect that the thermally induced magnetic fluctuations at the electron scales can be a relevant contribution to the magnetic variations observed in the solar wind and magnetosphere, but the calculations of these fluctuations near the threshold boundary needs to be confirmed for the electrons in and for both environments. Comparison between the solar wind and magnetosphere cases suggests that the results are not very sensitive to the ratio of $\omega_{pe}/|\Omega_e|$. The results presented here and motivated in combination by the observations of *Bale et al.* [2009] and *Kasper et al.* [2002], and the theoretical ideas by *Araneda et al.* [2012], *Viñas et al.* [2014], and *Navarro et al.* [2014], may lead us to a better understanding of the threshold conditions of magnetic fluctuations and nonthermal plasmas in the space environments. Full-particle numerical (PIC) simulation of the magnetic fluctuation will be presented in a subsequent paper to be compared with the results presented here, but preliminary results suggest similar conclusions. A generalization of the concepts presented here for the Tsallis-kappa-like distribution with thermal anisotropy, differential streaming, and multicomponent population cases are being carried out at present including oblique propagation and should reveal interesting comparisons with simulation results for parallel and obliquely propagating fluctuations.

Acknowledgments

A. F. Vinas would like to thank the NASA's Wind/SWE program for the support of this research. We also thank the Comisión Nacional de Ciencia y Tecnología (CONICyT, Chile) by providing financial support for postdoctoral (P. S. Moya) and doctoral (R. Navarro) fellows. We would like to thank FONDECYT 1110880 (J. A. Araneda), 3150262 (R. E. Navarro), 1121144 (V. Muñoz), and 1110135, 1110729, and 1130273 (J. A. Valdivia) for providing financial support. The results of this paper do not require any spacecraft data analysis, but the numerical data generated to reproduce all the figures will be made available upon request.

Michael Balikhin thanks the reviewers for their assistance in evaluating this paper.

References

Araneda, J., H. Astudillo, and E. Marsch (2012), Interactions of Alfvén-cyclotron waves with ions in the solar wind, *Space. Sci. Rev.*, *172*, 361–372, doi:10.1007/s11214-011-9773-0.

Bale, S. D., J. C. Kasper, G. G. Howes, E. Quataert, C. Salem, and D. Sundkvist (2009), Magnetic fluctuation power near proton temperature anisotropy instability thresholds in the solar wind, *Phys. Rev. Lett.*, *103*, 211101, doi:10.1103/PhysRevLett.103.211101.

Callen, H. B., and T. A. Welton (1951), Irreversibility and generalized noise, *Phys. Rev.*, *83*, 34–40, doi:10.1103/PhysRev.83.34.

Chame, A., and E. V. L. de Mello (1994), The fluctuation-dissipation theorem in the framework of the Tsallis statistics, *J. Phys. A: Math. Gen.*, *27*(11), 3663, doi:10.1088/0305-4470/27/11/016.

Chapman, D. A., and D. O. Gericke (2011), Analysis of Thomson scattering from nonequilibrium plasmas, *Phys. Rev. Lett.*, *107*, 165004, doi:10.1103/PhysRevLett.107.165004.

Christon, S. P., D. J. Williams, D. G. Mitchell, L. A. Frank, and C. Y. Huang (1989), Spectral characteristics of plasma sheet ion and electron populations during undisturbed geomagnetic conditions, *J. Geophys. Res.*, *94*, 13,409–13,424, doi:10.1029/JA094iA10p13409.

Feldman, W. C., J. R. Asbridge, S. J. Bame, M. D. Montgomery, and S. P. Gary (1975), Solar wind electrons, *J. Geophys. Res.*, *80*(31), 4181–4196, doi:10.1029/JA080i031p04181.

Felten, T., and R. Schlickeiser (2013a), Spontaneous electromagnetic fluctuations in unmagnetized plasmas. IV. Relativistic form factors of aperiodic Lorentzian modes, *Phys. Plasmas*, *20*, 082116, doi:10.1063/1.4817804.

Felten, T., and R. Schlickeiser (2013b), Spontaneous electromagnetic fluctuations in unmagnetized plasmas. V. Relativistic form factors of weakly damped/amplified thermal modes, *Phys. Plasmas*, *20*, 082117, doi:10.1063/1.4817805.

Felten, T., R. Schlickeiser, P. H. Yoon, and M. Lazar (2013), Spontaneous electromagnetic fluctuations in unmagnetized plasmas. II. Relativistic form factors of aperiodic thermal modes, *Phys. Plasmas*, *20*, 052113, doi:10.1063/1.4804402.
Fried, B. D., and S. D. Conte (1961), *The Plasma Dispersion Function*, Academic Press, San Diego, Calif.
Gell-Mann, M., and C. Tsallis (Eds.) (2004), *Nonextensive Entropy*, Oxford Univ. Press, New York.
Ichimaru, S. (1962), Theory of fluctuations in a plasma, *Ann. Phys.*, *20*, 78–118, doi:10.1016/0003-4916(62)90117-3.
Issautier, K., M. Moncuquet, N. Meyer-Vernet, S. Hoang, and R. Manning (2001), Quasi-thermal noise diagnostics in space plasmas, *Astrophys. Space Sci.*, *277*(1–2), 309–311, doi:10.1023/A:1012281730151.
Kasper, J. C., A. J. Lazarus, and S. P. Gary (2002), Wind/SWE observations of firehose constraint on solar wind proton temperature anisotropy, *Geophys. Res. Lett.*, *29*(17), 1839, doi:10.1029/2002GL015128.
Lazar, M., P. H. Yoon, and R. Schlickeiser (2012), Spontaneous electromagnetic fluctuations in unmagnetized plasmas. III. Generalized kappa distributions, *Phys. Plasmas*, *19*, 122108, doi:10.1063/1.4769308.
Lund, E. J., J. LaBelle, and R. A. Treumann (1994), On quasi-thermal fluctuations near the plasma frequency in the outer plasmasphere: A case study, *J. Geophys. Res.*, *99*(A12), 23,651–23,660, doi:10.1029/94JA02134.
Mace, R. L., and R. D. Sydora (2010), Parallel whistler instability in a plasma with an anisotropic bi-kappa distribution, *J. Geophys. Res.*, *115*, A07206, doi:10.1029/2009JA015064.
Maksimovic, M., V. Pierrard, and P. Riley (1997), Ulysses electron distributions fitted with kappa functions, *Geophys. Res. Lett.*, *24*(9), 1151–1154, doi:10.1029/97GL00992.
Meyer-Vernet, N., P. Couturier, S. Hoang, J. L. Steinberg, and R. D. Zwickl (1986), Ion thermal noise in the solar wind: Interpretation of the "excess" electric noise on ISEE 3, *J. Geophys. Res.*, *91*(A3), 3294–3298, doi:10.1029/JA091iA03p03294.
Meyer-Vernet, N., S. Hoang, K. Issautier, M. Moncuquet, and G. Marcos (2013), *Plasma Thermal Noise: The Long Wavelength Radio Limit*, pp. 67–74, AGU, Washington, D. C., doi:10.1029/GM119p0067.
Moncuquet, M., A. Lecacheux, N. Meyer-Vernet, B. Cecconi, and W. Kurth (2005), Quasi thermal noise spectroscopy in the inner magnetosphere of Saturn with Cassini/RPWS: Electron temperatures and density, *Geophys. Res. Lett.*, *32*, L20S02, doi:10.1029/2005GL022508.
Montgomery, M. D. (1968), Observations of electrons in the Earth's magnetotail by Vela Launch 2 satellites, *J. Geophys. Res.*, *73*(3), 871–889, doi:10.1029/JA073i003p00871.
Navarro, R. E., P. S. Moya, V. Muñoz, J. A. Araneda, A. F. Viñas, and J. A. Valdivia (2014), Solar wind thermally induced magnetic fluctuations, *Phys. Rev. Lett.*, *112*, 245001, doi:10.1103/PhysRevLett.112.245001.
Navarro, R. E., V. Muñoz, J. A. Araneda, A. F. Viñas, P. S. Moya, and J. A. Valdivia (2015), Magnetic Alfvén-cyclotron fluctuations of anisotropic non-thermal plasmas, *J. Geophys. Res. Space Physics*, *120*, doi:10.1002/2014JA020550, in press.
Nieves-Chinchilla, T., and A. F. Viñas (2008), Solar wind electron distribution functions inside magnetic clouds, *J. Geophys. Res.*, *113*, A02105, doi:10.1029/2007JA012703.
Olbert, S. (1968), *Summary of Experimental Results From M. I. T. Detector on IMP-1, Astrophys. Space Sci. Libr.*, pp. 641–659, Springer, Netherlands, doi:10.1007/978-94-010-3467-8_23.
Pilipp, W. G., H. Miggenrieder, M. D. Montgomery, K. H. Mühlhäuser, H. Rosenbauer, and R. Schwenn (1987), Unusual electron distribution functions in the solar wind derived from the Helios Plasma Experiment: Double-Strahl distributions and distributions with an extremely anisotropic core, *J. Geophys. Res.*, *92*(A2), 1093–1101, doi:10.1029/JA092iA02p01093.
Rajagopal, A. K. (1996), Dynamic linear response theory for a nonextensive system based on the Tsallis prescription, *Phys. Rev. Lett.*, *76*, 3469–3473, doi:10.1103/PhysRevLett.76.3469.
Schlickeiser, R., and P. H. Yoon (2012), Spontaneous electromagnetic fluctuations in unmagnetized plasmas I: General theory and nonrelativistic limit, *Phys. Plasmas*, *19*, 022105, doi:10.1063/1.3682985.
Sitenko, A. (1967), *Electromagnetic Fluctuations in Plasma*, Academic Press, San Diego, Calif.
Stverak, S., P. Trávníček, M. Maksimovic, E. Marsch, A. N. Fazakerley, and E. E. Scime (2008), Electron temperature anisotropy constraints in the solar wind, *J. Geophys. Res.*, *113*, A03103, doi:10.1029/2007JA012733.
Summers, D., and R. M. Thorne (1991), The modified plasma dispersion function, *Phys. Fluids B*, *3*(8), 1835–1847, doi:10.1063/1.859653.
Tsallis, C. (1988), Possible generalization of Boltzmann-Gibbs statistics, *J. Stat. Phys.*, *52*, 479–487.
Tsallis, C. (2009), *Introduction to Nonextensive Statistical Mechanics*, Springer, Berlin.
Tsallis, C., and E. Brigatti (2004), Nonextensive statistical mechanics: A brief introduction, *Continuum Mech. Thermodyn.*, *16*, 223–235, doi:10.1007/s00161-004-0174-4.
Vasyliunas, V. M. (1968), A survey of low-energy electrons in the evening sector of the magnetosphere with OGO 1 and OGO 3, *J. Geophys. Res.*, *73*(9), 2839–2884, doi:10.1029/JA073i009p02839.
Viñas, A. F., R. L. Mace, and R. F. Benson (2005), Dispersion characteristics for plasma resonances of Maxwellian and kappa distribution plasmas and their comparisons to the IMAGE/RPI observations, *J. Geophys. Res.*, *110*, A06202, doi:10.1029/2004JA010967.
Viñas, A. F., P. S. Moya, R. Navarro, and J. A. Araneda (2014), The role of higher-order modes on the electromagnetic whistler-cyclotron wave fluctuations of thermal and non-thermal plasmas, *Phys. Plasmas*, *21*, 012902, doi:10.1063/1.4861865.
Zouganelis, I. (2008), Measuring suprathermal electron parameters in space plasmas: Implementation of the quasi-thermal noise spectroscopy with kappa distributions using in situ Ulysses/URAP radio measurements in the solar wind, *J. Geophys. Res.*, *113*, A08111, doi:10.1029/2007JA012979.